# Calculating rate constants for intersystem crossing and internal conversion in the Franck-Condon and Herzberg-Teller approximations

Valiev, Rashid R.

2019-09-14

Valiev , R R , Cherepanov , V N , Nasibullin , R T , Sundholm , D & Kurten , T 2019 , ' Calculating rate constants for intersystem crossing and internal conversion in the Franck-Condon and Herzberg-Teller approximations ' , Physical Chemistry Chemical Physics , vol. 21 , no. 34 , pp. 18495-18500 . https://doi.org/10.1039/c9cp03183a

http://hdl.handle.net/10138/318127
https://doi.org/10.1039/c9cp03183a

Journal Name

ARTICLE TYPE

Cite this: DOI: 00.0000/xxxxxxxxxx

# Calculating rate constants for intersystem crossing and internal conversion in the Franck-Condon and Herzberg-Teller approximations†

Rashid R. Valiev,*[a,b] Victor N. Cherepanov,[a] Rinat T. Nasibullin,[a] Dage Sundholm,[c] and Theo Kurten[b]

Received Date
Accepted Date

DOI: 00.0000/xxxxxxxxxx

**Effective and fast algorithms for calculating rate constants for internal conversion (IC) and intersystem crossing (ISC) in the Franck-Condon and Herzberg-Teller approximations have been developed and implemented. The methods have been employed for calculating IC and ISC rate constants for the pyrromethene-567 dye (PM567), hetero[8]circulene (4B) and free-base porphyrin ($H_2P$). The fluorescence quantum yields obtained by comparing calculated rate constants for the radiative and non-radiative processes are in good agreement with experimental data.**

## Introduction

Photophysical processes comprise transition probabilities or rate constants for transitions between molecular electronic states.[1,2] The ratio between the rate constants for the radiative and non-radiative electronic transitions provides information about the fluorescence and phosphorescence quantum yields, which are important for the design of light emitting diodes,[3,4] laser dye devices,[5,6] photodynamic therapy,[7,8] and for understanding physical and chemical processes in the atmosphere.[9] The gas-phase formation of low-volatility accretion products, which is a key process affecting aerosol concentrations of importance for the air quality and the climate, most likely involve intersystem crossings.[9–11] Rate constants for radiative intramolecular electronic transitions can nowadays be calculated with rather high accuracy, whereas calculations of the rate constants for non-radiative processes are more complicated.[1,12,13] The main non-radiative processes are intersystem crossing (ISC) and internal conversion (IC), which are transitions between two electronic states with different and the same spin multiplicity, respectively.[1,12] The rate constants of the IC and ISC processes can be obtained by using molecular dynamics simulations and *ab initio* methods,[14–16] which are computationally challenging implying that alternative approaches are needed.[1]

Recently, we developed an effective algorithm based on the original works of Bixon, Jortner and Plotnikov *et al.*,[17,18] who developed methods for calculating IC and ISC rate constants ($k_{IC}$ and $k_{ISC}$) at *ab initio* levels of theory.[12] We previously used these methods for calculating the $k_{IC}$ and $k_{ISC}$ rate constants for organic and organometallic compounds such as the pyrromethene-567 dye (PM567), psoralene, hetero[8]circulenes (4B), free-base porphyrin ($H_2P$), naphthalene, fac−$Alq_3$, fac−$Ir(ppy)_3$ and polyacenes.[12] The rate constants were calculated in the Franck-Condon (FC) approximation and the obtained values agreed in most cases well with experimental data. Exceptions were the rate constants for $H_2P$ and polyacenes. We found that one has to go beyond adiabatic approximation in order to obtained accurate rate constants for the polyacenes,[12] whereas the $k_{IC}$ and $k_{ISC}$ rate constants for $H_2P$ were significantly underestimated due to the use of the FC approximation.

Here, we present modifications of our algorithm to calculate rate constants by extending it to the Herzberg-Teller (HT) approximation, where one also considers that the electronic transition dipole moments depend on the nuclear coordinates.[19] Calculations of $k_{IC}$ and $k_{ISC}$ with the modified version of the algorithm of this work are very fast taking about 10-20 seconds on a single processor even for the largest molecules studied in this work. We have calculated $k_{IC}$ and $k_{ISC}$ for 4B, $H_2P$, and PM567 in the FC and HT approximations. We chose these molecules, because they have completely different photophysical properties and they are

[a] *Tomsk State University, Lenin Avenue 36, Tomsk 634050, Russia.*
[b] *University of Helsinki, Institute for Atmospheric and Earth System Research, Faculty of Science, FIN-00014 University of Helsinki, Finland.*
[c] *University of Helsinki, Department of Chemistry, Faculty of Science, P.O. Box 55 (A.I. Virtanens plats 1), FIN-00014 University of Helsinki, Finland.*

† Electronic Supplementary Information (ESI) available: Detailed description of the electronic structure methods and the Cartesian coordinates of the atomic positions of the studied molecules are given. See DOI: 10.1039/x0xx00000x.

important in many applications.[3–8]

## Theory

In the theory of Plotnikov and Jortner *et al.*[17,18,20] the general expression for calculating rate constants of non-radiative transitions ($k_{\rm nr}$) such as $k_{IC}$ and $k_{ISC}$ is (in atomic units):

$$k_{\rm nr} = \frac{4}{\Gamma_f}\sum_n |V_{i0,fn}|^2 \tag{1}$$

where $i$ is the initial electronic state, $n$ is a vibrational level of the final state ($f$), $\Gamma_f$ is the relaxation width of $f$, and $V_{i0,fn}$ is the matrix element of the perturbation operator discussed below. Only the lowest vibrational state of $i$ has to be considered at room temperature. Eqn (1) holds when $k_{\rm nr} \ll \Gamma_f$. $\Gamma_f$ is generally of the order of $10^{14}$ $s^{-1}$, which is much larger than the $k_{\rm nr}$ of about $10^7 - 10^{12}$ $s^{-1}$,[12] implying that the condition $k_{\rm nr} \ll \Gamma_f$ is often fulfilled.

In the adiabatic approximation, the matrix elements of the perturbation operator for calculation of $k_{ISC}$ are given by:[12]

$$V_{i0,fn} = \langle\langle \phi_i(\vec{r},\vec{s},\vec{R})\chi_{i0}(\vec{R})\hat{H}_{SO}(\vec{r},\vec{s})\phi_f(\vec{r},\vec{s},\vec{R})\chi_{fn}(\vec{R})\rangle\rangle. \tag{2}$$

The corresponding matrix elements for calculating $k_{IC}$ are:[12]

$$\begin{aligned} V_{i0,fn} &= \langle\langle \phi_i(\vec{r},\vec{s},\vec{R})\chi_{i0}(\vec{R})\hat{V}\phi_f(\vec{r},\vec{s},\vec{R})\chi_{fn}(\vec{R})\rangle\rangle \\ &= -\sum_v\sum_q (2M_v)^{-1}\langle\langle \phi_i(\vec{r},\vec{s},\vec{R})\chi_{fn}(\vec{R})\chi_{i0}(\vec{R})\frac{\partial^2}{\partial R_{vq}^2}\phi_f(\vec{r},\vec{s},\vec{R})\rangle\rangle \\ &\quad -\sum_v\sum_q M_v^{-1}\langle\langle \phi_i(\vec{r},\vec{s},\vec{R})\chi_{i0}(\vec{R})\frac{\partial\phi_f(\vec{r},\vec{s},\vec{R})}{\partial R_{vq}}\frac{\partial\chi_{fn}(\vec{R})}{\partial R_{qv}}\rangle\rangle \end{aligned} \tag{3}$$

In eqn (2) and (3), $\phi_i(\vec{r},\vec{s},\vec{R})$ and $\chi(\vec{R})$ are electronic and nuclear wavefunctions, $M_v$ is mass of $v$-*th* nucleus, $q$=*x,y,z*, $R_{vq}$ are the Cartesian coordinates of the $v$-*th* nucleus, $\vec{r}$ and $\vec{s}$ are the space and spin electronic coordinates. $\hat{H}_{SO}(\vec{r},\vec{s})$ consists of one-electron and two-electron spin-orbit coupling terms.[1,12] The double brackets denote that the integration is performed over the electronic and the nuclear coordinates. The harmonic approximation is generally sufficiently accurate, when considering the lowest electronic excited states.[12] When the Duschinsky mixing[21] of the normal coordinates of the initial and final states can be neglected and the frequencies of harmonic oscillator are similar for initial and final electronic states, the electronic matrix elements can be easily expanded into a Taylor series. By considering only the two first terms in the series expansion, the expressions for $k_{IC}$ and $k_{ISC}$ become:

$$k_{ISC} = \frac{4}{\Gamma_f}\sum_{n_1,n_2,..,n_{3N-6}}^{Comb}\left(H_{SO}^{if}|_{\vec{R}=\vec{R}_0}\left[\prod_{k=1}^{3N-6}\left(\frac{e^{-y_k}y_k^{n_k}}{n_k!}\right)^{1/2}\right] + \sum_{j=1}^{3N-6} t_j W_j\cdot\left[\prod_{\substack{k=1\\k\neq j}}^{3N-6}\left(\frac{e^{-y_k}y_k^{n_k}}{n_k!}\right)^{1/2}\right]\right)^2 \tag{4}$$

$$k_{IC} = \frac{4}{\Gamma_f}\sum_{n_1,n_2,..,n_{3N-6}}^{Comb}$$

$$\left(D\prod_{k=1}^{3N-6}\left(\frac{e^{-y_k}y_k^{n_k}}{n_k!}\right)^{1/2} + \left[\sum_{j=1}^{3N-6} d_j\cdot b_j\prod_{\substack{k=1\\k\neq j}}^{3N-6}\left(\frac{e^{-y_k}y_k^{n_k}}{n_k!}\right)^{1/2}\right] + \sum_j\sum_{j'} b_j t_{j'} W_{jj'}\cdot\prod_{\substack{k=1\\k\neq j\\k\neq j'}}^{3N-6}\left(\frac{e^{-y_k}y_k^{n_k}}{n_k!}\right)^{1/2}\right)^2 \tag{5}$$

In eqn (4) and (5), *Comb* denotes that the summation runs over a limited number of linear combinations of the vibrational modes, which fulfill within an energy margin of 200 $cm^{-1}$ the energy-conservation condition $E_{if} = n_1\omega_1 + n_2\omega_2 + \ldots + n_{3N-6}\omega_{3N-6}$, since the electronic excitation energy ($E_{if}$) is assumed to be transfered to a combination of vibrational modes with the different excitation levels ($n_1, n_2, \ldots$). The chosen energy margin of 200 $cm^{-1}$ is based on the estimated maximum error of the harmonic approximation of the vibrational frequency calculations. $H_{SO}^{if}|_{\vec{R}=\vec{R}_0}$ denotes the matrix elements of the spin-orbit coupling interaction calculated using the equilibrium geometry ($\vec{R}=\vec{R}_0$) of the initial electronic state. The expressions for the other terms in eqn (4) and (5) are:

$$W_j = \sum_v\sum_q \frac{\partial H_{SO}^{if}}{\partial R_{vq}}\bigg|_{\vec{R}=\vec{R}_0} M_v^{-1/2}L_{vqj} \tag{6}$$

$$W_{jj'} = -\sum_{v,v'}\sum_{q,q'}\langle\frac{\phi_i(\vec{r},\vec{s},\vec{R})\partial^2\phi_f(\vec{r},\vec{s},\vec{R})}{\partial R_{vq}\partial R_{v'q'}}\rangle\bigg|_{\vec{R}=\vec{R}_0} M_v^{-1/2}M_{v'}^{-1/2}L_{vqj}L_{v'q'j'} \tag{7}$$

$$D = -\sum_v\sum_q (2M_v)^{-1}\langle\phi_i(\vec{r},\vec{s},\vec{R})|\frac{\partial^2}{\partial R_{vq}^2}|\phi_f(\vec{r},\vec{s},\vec{R})\rangle\bigg|_{\vec{R}=\vec{R}_0} \tag{8}$$

$$d_j = -\sum_v\sum_q M_v^{-1/2}L_{vqj}\langle\phi_i(\vec{r},\vec{s},\vec{R})|\frac{\partial\phi_f(\vec{r},\vec{s},\vec{R})}{\partial R_{vq}}\rangle\bigg|_{\vec{R}=\vec{R}_0} \tag{9}$$

$$\begin{aligned} t_j &= \langle\chi_{i0_j}(Q_j)|Q_j|\chi_{fn_j}(Q_j)\rangle \\ &= \left[\frac{1}{2\omega_j n_j!}(n_j+y_j)^2\cdot e^{-y_j}\cdot y_j^{n_j-1}\right]^{1/2} \end{aligned} \tag{10}$$

$$\begin{aligned} b_j &= \langle\chi_{i0_j}(Q_j)|\frac{\partial}{\partial Q_j}|\chi_{fn_j}(Q_j)\rangle \\ &= \left[\frac{1}{2n_j!}\omega_j(n_j-y_j)^2\cdot e^{-y_j}\cdot y_j^{n_j-1}\right]^{1/2} \end{aligned} \tag{11}$$

$$y_j = \frac{1}{2}\omega_j\cdot\left|Q_{0_j}^f - Q_{0_j}^i\right|^2 \tag{12}$$

where $Q_j$ are the normal coordinates. $Q_{0_j}^i$ and $Q_{0_j}^f$ are the coordinates of the equilibrium positions of $j$-*th* harmonic oscillator, $L_{vqj}$ are coefficients of the linear relation between the Cartesian and the normal coordinates ($R_{vq} - R_{0vq} = M_v^{-1/2}L_{vqj}Q_j$), $\omega_j$ is the frequency of the $j$-*th* harmonic oscillator, and $y_j$ are the Huang-Rhys factors. The derivatives in eqn (6)-(9) are calculated numerically using a three-point finite-difference approximation with a step length of 0.05 Å along each Cartesian coordinate.

The expressions in eqn (4) and (5) can be simplified by considering only the most significant terms in the $E_{if} = n_1\omega_1 + n_2\omega_2 + \ldots + n_{3N-6}\omega_{3N-6}$ summation. The approximate expressions for

calculating the rate constants are then

$$k_{IC-FC} = \frac{4}{\Gamma_f}\sum_{j=1}^{3N-6}(d_j \cdot b_j\sqrt{P_j})^2; P_j = \sum_{n_1,n_2,..,n_{3N-6}}^{Comb}\prod_{\substack{k=1\\k\neq j}}^{3N-6}(\frac{e^{-y_k}y_k^{n_k}}{n_k!}) \quad (13)$$

$$k_{IC-HT} = \frac{4}{\Gamma_f}\sum_{j}\sum_{j'}(b_j t_{j'} W_{jj'}\sqrt{P_{jj'}})^2; P_{jj'} = \sum_{n_1,n_2,..,n_{3N-6}}^{Comb}\prod_{\substack{k=1\\k\neq j\\k\neq j'}}^{3N-6}(\frac{e^{-y_k}y_k^{n_k}}{n_k!}) \quad (14)$$

$$k_{ISC-FC} = \frac{4}{\Gamma_f}\left(H_{SO}^{if}|_{\vec{R}=\vec{R}_0}\right)^2 P;\ P = \sum_{n_1,n_2,..,n_{3N-6}}^{Comb}\prod_{k=1}^{3N-6}(\frac{e^{-y_k}y_k^{n_k}}{n_k!}) \quad (15)$$

$$k_{ISC-HT} = \frac{4}{\Gamma_f}\sum_{j=1}^{3N-6}(t_j W_j\sqrt{P_j})^2; P_j = \sum_{n_1,n_2,..,n_{3N-6}}^{Comb}\prod_{\substack{k=1\\k\neq j}}^{3N-6}(\frac{e^{-y_k}y_k^{n_k}}{n_k!}) \quad (16)$$

In the eqn (13)-(16), the summation over the excitation modes $(n_1\omega_1 + n_2\omega_2 + ..n_{3N-6}\omega_{3N-6})$ is separated and grouped into $P$, $P_j$ and $P_{jj'}$, which consist of a summation of the FC factors and depend on the energy gap. The $t_j$ and $b_j$ terms in eqn (13), (14) and (16) account for the energy of the $n_j$-th excitation of vibrational mode $j$ and the energy of the $n_{j'}$-th excitation of vibrational mode $j'$. The energy conservation condition for the calculation of $P_j$ and $P_{j,j'}$ becomes then $E_{if} - n_j\omega_j = n_1\omega_1 + n_2\omega_2 + ..n_{3N-6}\omega_{3N-6}$ and $E_{if} - n_j\omega_j - n_{j'}\omega_{j'} = n_1\omega_1 + n_2\omega_2 + ..n_{3N-6}\omega_{3N-6}$, respectively.

The universal $P$ functions plotted in Figure 1 can be used for estimating $P_j$ and $P_{jj'}$ that appear in eqn (13), (14) and (16). The criteria for using the different fitting curves, which are based on the values of the Huang-Rhys factors ($y$) for the higher frequency modes are:

1. when at least one vibrational mode has >1000 $cm^{-1}$ and $0.5 > y > 0.1$, curve A is used.
2. when there is no vibrational mode with >1000 $cm^{-1}$ and $y > 0.1$, curve B is used.
3. when one vibrational mode has $y > 0.5$, curve C is used.

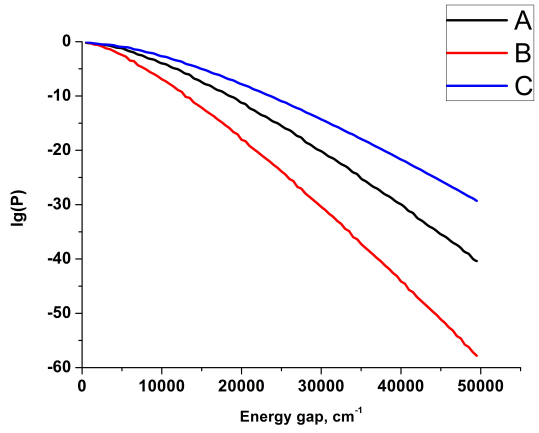


**Fig. 1** The A, B, and C curves given as $\log_{10}$(P) are shown as a function of the energy difference between the electronic states (in $cm^{-1}$).

Curve A is similar to the fitting curve used by Plotnikov.[18]

The PM567, $H_2P$ and 4B molecules shown in Figure 2 have been studied in this work, because they belong to case 1), 2) and 3), respectively. The error bars of the rate constants calculated using eqn (13)-(16) are 30-70%. The A, B, C curves can be obtained by using modes with vibrational energies satisfying the energy condition $n_1\omega_1 + n_2\omega_2 + \ldots + n_{3N-6}\omega_{3N-6} = E_{if}$ and the corresponding $y$ values. The A curve was obtained by using two vibrational modes whose energies are 1400 $cm^{-1}$ ($y = 1.0$) and 400 $cm^{-1}$ ($y = 0.3$). The B curve is obtained using two modes with vibrational energies of 1400 $cm^{-1}$ ($y = 0.3$) and 400 $cm^{-1}$ ($y = 0.6$). The C curve is constructed by using vibrational energies of three modes whose energies are 1400 $cm^{-1}$ ($y = 1.0$), 400 $cm^{-1}$ ($y = 0.6$), and 1700 $cm^{-1}$ ($y = 1.0$).

The fluorescence quantum yield ($\gamma_{fl}$) was calculated from the rate constants using

$$\gamma_{fl} = \frac{k_r}{k_r + \sum_j k_{ISCj} + k_{IC}}, \quad (17)$$

where $k_r$ is the radiative rate constant and the $k_{ISCj}$ are $k_{ISC}$ the rate constant of the intersystem crossing from the $S_1$ state to the *j-th* excited electronic triplet state, which is energetically below $S_1$.

## Computaional details

The molecular structures of the first excited electronic singlet state ($S_1$) of the studied molecules were optimized with Gaussian-09 at the time dependent density functional theory level using the B3LYP exchange-correlation functional and def2-TZVP basis sets.[22–26]

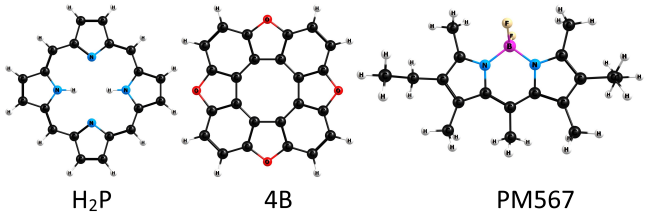


**Fig. 2** The molecular structures of $H_2P$, 4B and PM567.

Calculations of the electronic excitation energies were carried out with Firefly at the extended multi-configuration quasi-degenerate perturbation theory level of second order (XMC-QDPT2).[27,28] The computational details and the Cartesian coordinates of the atomic positions of the optimized molecular structures are given as electronic supplementary information (ESI)†.

The electronic excitation energies of the lowest singlet and triplet states calculated at the XMC-QDPT2 level of theory are given as electronic supplementary information (ESI). The matrix elements of the spin-orbit coupling interaction are also reported in the ESI and discussed in more detail in the recent work of Valiev *et al.*[12]

## Results and discussion

The rate constants $k_{IC}$ and $k_{ISC}$ for $H_2P$, 4B, and PM567 have been calculated in the FC and HT approximations by using eqn

(4) and (5). The obtained results are given in Table 1. The FC and HT contributions to $k_{IC}$ and $k_{ISC}$ are also reported in Table 1.

In a previous study, we noted that the vibrational combinations $n_1\omega_1 + n_2\omega_2 + \ldots + n_{3N-6}\omega_{3N-6}$ involving the X-H modes contribute significantly to the $k_{IC-FC}$ rate constants because of their large vibrational energy and small $y$ values that lead to large $b_j$ factors.[12] The contributions from other vibrational modes originate from $\prod_{\substack{k=1 \\ k\neq j}}^{3N-6} \left(\frac{e^{-y_k} y_k^{n_k}}{n_k!}\right)^{1/2}$. The combination of two X-H modes in the $b_j$ and $t_{j'}$ factors lead to large contributions to the $k_{IC-HT}$ rate constants of PM567, $H_2P$ and 4B. Thus, the X-H modes yield large contributions to the rate constants in the FC and HT approximations. The out-of-plane modes of $H_2P$, belonging to the $b_{2g}$ and $b_{3g}$ irreducible representations and the $a_{2g}$ modes of 4B and PM567 contribute significantly to the $k_{ISC-HT}$ rate constants. These vibrational modes are shown for the molecular structure of the $S_0$ state in Figure 3. The importance of the $b_{2g}$ and $b_{3g}$ modes of $H_2P$ has been previously discussed by Perun *et al.*[29] For 4B, the corresponding vibrational modes at 258 $cm^{-1}$ and 639 $cm^{-1}$ have small contributions of $< 10^{-3}$ $s^{-1}$ to the $k_{ISC-HT}$ rate constant. The $k_{ISC_1}$ and $k_{ISC_2}$ rate constants practically vanish at the HT level, whereas the $a_{2g}$ modes of PM567 with vibrational energies of 326 $cm^{-1}$, 412 $cm^{-1}$ and 692 $cm^{-1}$ yield large contributions to the $k_{ISC-HT}$ rate constants.

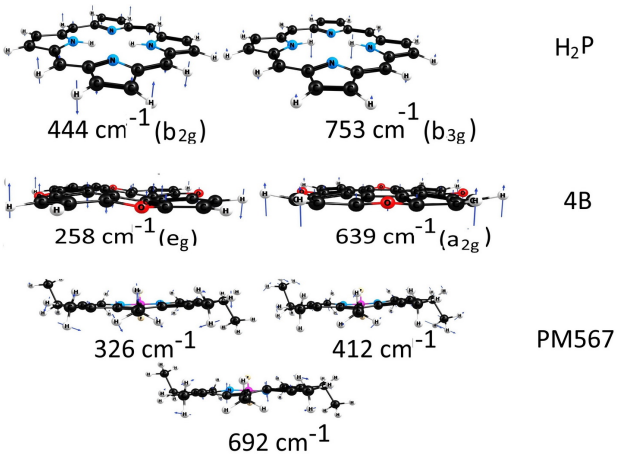


**Fig. 3** Vibrational modes giving large contributions to the $k_{ISC-HT}$ rate constants of $H_2P$, 4B and PM567.

The calculated $k_{IC}$ and $k_{ISC}$ rate constants for $H_2P$ differ significantly when using the FC and the HT approximation, respectively. The *ISC* rate constant at the HT level ($k_{ISC-HT}$) is $7 \cdot 10^6$ $s^{-1}$, which agrees well with the previously calculated value of about $10^7$ $s^{-1}$.[30] The calculated values for $k_{ISC}$ and $k_{IC}$ in the HT approximation combined with the rate constant of the radiative transition ($k_r$) of $5 \cdot 10^6$ $s^{-1}$ result in a quantum yield of fluorescence ($\gamma_{fl}$) of 0.08, which agrees well with the experimental value of 0.05.[8] The obtained values for $k_{ISC}$ and $k_{IC}$ at the HT level agree well with the previously calculated values for $k_{ISC}$ of $0.9 \cdot 10^8$ $s^{-1}$ and $k_{IC}$ of $1 \cdot 10^8$ $s^{-1}$, which were obtained by using $V_{i0,fn}$ values calculated at semi-empirical level of theory.[31] The calculations show that the electronic excitation energy of the first excited singlet state ($S_1$) of $H_2P$ decays almost equally fast through the ISC and IC channels. The calculated values for $k_{ISC1}$ in the HT and FC approximations are different for PM567 since the rate constant for intersystem crossing ($k_{ISC-FC}$) is severely underestimated at the FC level. The contributions from the one-electron and two-electron spin-orbit operators are of the same size with opposite sign implying that the total spin-orbit contribution is small as one would also expect for the organic molecules consisting of only light elements.[1,32] When there is at least one vibrational mode with $\omega$>1000 $cm^{-1}$ and $y$>0.1, the HT contribution and the two-electron SO contribution in eqn (4) are of the same order of magnitude, but with opposite sign. The one-electron spin-orbit term is then the main contribution to $k_{ISC-HT}$. We used this approximation in a previous work for calculating the $k_{ISC}$ rate constants for a number of organic and organometallic compounds.[4,12,33,34]

**Table 1** The $k_{IC}$ and $k_{ISC}$ rate constants (in $s^{-1}$) for the $S_1 \rightarrow S_0$, $S_1 \rightarrow T_1$ and $S_1 \rightarrow T_2$ transitions of $H_2P$, 4B and PM567 calculated at the FC and HT levels. The quantum yields of fluorescence ($\gamma_{fl}$) calculated at the FC and HT levels are compared to experimental values. The vibrational energy (in $cm^{-1}$) of the most relevant modes with $y$ > 0.1 are also given.

| | $H_2P$ | | 4B | | PM567 | |
|---|---|---|---|---|---|---|
| | FC | HT | FC | HT | FC | HT |
| $k_{ISC_1}$ | $3 \cdot 10^2$ | $7 \cdot 10^6$ | 0.0 | 0.0 | $4 \cdot 10^3$ | $1 \cdot 10^6$ |
| $k_{ISC_2}$ | 0.0 | 0.0 | 0.0 | 0.0 | $5 \cdot 10^6$ | $8 \cdot 10^6$ |
| $k_{IC}$ | $1 \cdot 10^3$ | $8 \cdot 10^7$ | $6 \cdot 10^7$ | $5 \cdot 10^6$ | $7 \cdot 10^4$ | $1 \cdot 10^6$ |
| $k_r$ | $5 \cdot 10^6$ | | $9 \cdot 10^6$ | | $4 \cdot 10^7$ | |
| $\gamma_{fl}$ | 0.99 | 0.08 | 0.13 | 0.13 | 0.79 | 0.77 |
| $\gamma_{fl}$ (Exp.) | 0.05[a] | | 0.09[b] | | 0.9[b] | |
| $\omega$ | | | 1276;1453 | | 1255 | |
| $y$ | | | 0.35; 0.19 | | 0.1 | |
| $\omega$ | | | 1536;1703 | | | |
| $y$ | | | 0.16; 0.84 | | | |

[a] The experimental value was taken from Ref. 8
[b] The experimental value was taken from Ref. 12

However, this approximation cannot be employed for $H_2P$. For 4B, the HT contribution to the rate constant for internal conversion ($k_{IC-HT}$) is one order of magnitude smaller than $k_{IC-FC}$, whereas for PM567 $k_{IC-HT} \approx k_{IC-FC}$.

The calculated quantum yields ($\gamma_{fl}$) for PM567 and 4B are 0.77 and 0.13, respectively, which agree well with the experimental $\gamma_{fl}$ values of 0.9 and 0.09 for PM567 and 4B, respectively. For 4B, we find that IC is the main channel for the decay of the electronic excitation energy of the $S_1$ state and mainly responsible for quenching of the fluorescence. For PM567, the radiative electronic transition is main decay channel from the $S_1$ state, which is reflected in the large quantum yield of fluorescence.

## Summary and discussion

The developed algorithm for fast calculations of the $k_{IC}$ and $k_{ISC}$ rate constatnts at FC and HT approximation is based on the following assumptions:

1) the adiabatic approximation
2) the harmonic approximation
3) the linear displacement approximation

Accurate fluorescence quantum yields were obtained for $H_2P$, 4B and PM567, because these assumptions are valid for them.

For non-rigid molecules, contributions due to the Duschinsky effect can be significant. The adiabatic approximation is accurate for most molecules; one known exception is polyacenes.[12] The vibrational modes associated with the X-H vibrations (X=O, C and N) contribute significantly to the $b_j$ values obtained at the FC and HT levels using eqn (11). These vibrational modes can also have large anharmonic effects.[18] Here, we estimated the contributions to $b_j$ from anharmonic effects by using vibrational wavefunctions of the Morse potential for the X-H stretch.[30] The calculations showed that the anharmonic contribution is only 5-8%, because the lowest vibrational mode ($n_j$=1) is the only one with a large contribution to $b_j$. Since the neglected Duschinsky effect can play an important role for the rate constants of non-radiative processes, we plan to extend the algorithm by considering the Duschinsky effect for studies of non-rigid molecules.

A main conclusion of this articles is that the spin-vibronic effects are important not only for the intersystem crossing (ISC) process[1,32] but also for internal conversion (IC).

## Acknowledgments

We thank for the support from Svenska Kulturfonden, grant numbers 136102 and 139379, and The Academy of Finland, grant numbers 1315600 and 131482, and the Magnus Ehrnrooth Foundation. The research was also supported by a grant from Russian Science Foundation (project No. 17-73-20012) CSC - the Finnish IT Center for Science as well as the Finnish Grid and Cloud Infrastructure (persistent identifier urn:nbn:fi:researchinfras-2016072533) are acknowledged for computer time.

## Notes and references

1 C. M. Marian, *Wiley Interdiscip. Comput. Mol. Sci.*, 2012, **2**, 187–203.

2 D. Beljonne, Z. Shuai, G. Pourtois and J. L. Bredas, *J. Phys. Chem. A*, 2001, **105**, 3899–3907.

3 B. F. Minaev, G. Baryshnikov and H. Ågren, *Phys. Chem. Chem. Phys.*, 2014, **16**, 1719–1758.

4 G. V. Baryshnikov, R. R. Valiev, N. N. Karaush, V. A. Minaeva, A. N. Sinelnikov, S. K. Pedersen, M. Pittelkow, B. F. Minaev and H. Ågren, *Phys. Chem. Chem. Phys*, 2016, **18**, 28040–28051.

5 R. Valiev, E. Telminov, T. A. Solodova, E. N. Ponyavina, R. M. Gadirov, G. V. Maier and T. N. Kopylova, *Chem. Phys. Lett.*, 2013, **588**, 184–187.

6 B. F. Minaev, R. R. Valiev, E. N. Nikonova, R. M. Gadirov, T. A. Solodova and T. N. Kopylova, *J. Phys. Chem. A*, 2015, **119**, 1948–1956.

7 N. G. Bryantseva, I. V. Sokolova, R. M. Gadirov, V. P. Khilya and L. Garazd, *J. Appl. Spectrosc*, 2009, **76**, 813–818.

8 D. Dolphin, *The Porphyrins*, Academic Press, New York, 1978.

9 R. R. Valiev, G. Hasan, V.-T. Salo, J. Kubecka and T. Kurten., *J. Phys. Chem. A*, 2019.

10 F. Bianchi, T. Kurten, M. Riva, C. Mohr, M. P. Rissanen, P. Roldin, T. Berndt, J. D. Crounse, P. O. Wennberg, T. F. Mentel, J. Wildt, H. Junninen, M. K. T. Jokinen, D. R. Worsnop, J. A. Thornton, N. Donahue, H. G. Kjaergaard and M. Ehn, *Chem. Rev.*, 2019, **119**, 3472–3509.

11 R. Lee, G. Gryn'ova, K. U. Ingold and M. L. Coote, *Phys. Chem. Chem. Phys.*, 2016, **18**, 23673–23679.

12 R. R. Valiev, V. N. Cherepanov, G. V. Baryshnikov and D. Sundholm., *Phys. Chem. Chem. Phys.*, 2018, **20**, 6121–6133.

13 S. J. Strickler and R. A. Berg, *Chem. Phys. Lett.*, 1964, **37**, 814–822.

14 W. Feng, L. Xu, X.-Q. Li, W. Fang and Y. Yan, *AIP Adv.*, 2014, **4**, 077131.

15 J. Cao and Z.-Z. Xie, *Phys. Chem. Chem. Phys.*, 2016, **18**, 6931–6945.

16 J. C. Vincenta and F. Furche, *Phys. Chem. Chem. Phys.*, 2013, **15**, 18336–18348.

17 M. Bixon and J. Jortner, *J. Chem. Phys.*, 1968, **48**, 715–726.

18 V. G. Plotnikov, V. A. Dolgikh and V. M. Komarov, *Opt. Spectrosc.*, 1977, **43**, 522–527.

19 G. Herzberg and E. Teller, *J. Phys. Chem. Abt. B*, 1933, **21**, 410–446.

20 R. Englman and J. Jortner, *Mol. Phys.*, 1970, **18**, 145–164.

21 F. Duschinsky, *Acta Physicochim. URSS*, 1937, **7**, 510.

22 *Gaussian09 Revision E.01*, Gaussian Inc. Wallingford CT 2009,https://gaussian.com.

23 M. E. Casida and M. Huix-Rotllant, *Annu. Rev. Phys.*, 2012, **63**, 287–323.

24 A. D. Becke, *J. Chem. Phys.*, 1993, **98**, 1372–1377.

25 C. Lee, W. Yang and R. G. Parr, *Phys. Rev. B*, 1988, **37**, 785–789.

26 F. Weigend and R. Ahlrichs, *Phys. Chem. Chem. Phys.*, 2005, **7**, 3297–3305.

27 A. A. Granovsky, *J. Chem. Phys.*, 2011, **134**, 214113.

28 A. A. Granovsky, *Firefly, 8.2.0*, http://classic.chem.msu.su/gran/firefly/index.html.

29 S. Perun, J. Tachen and C. M. Marian, *Chem. Phys. Chem.*, 1998, **9**, 282–292.

30 M. Bancewicz, *J. Phys. A: Math. Gen.*, 1998, **31**, 3461–3467.

31 R. R. Valiev, V. N. Cherepanov, V. Y. Artyukhov and D. Sundholm, *Phys. Chem. Chem. Phys.*, 2012, **14**, 11508–11517.

32 T. J. Penfold, E. Gindensperger, C. Daniel and C. M. Marian., *Chem. Rev*, 2018, **118**, 6975–7025.

33 G. V. Baryshnikov, R. R. Valiev, B. F. Minaev and H. Ågren, *New. J. Chem.*, 2017, **41**, 7621–7625.

34 R. R. Valiev, E. N. Telminov, T. A. Solodova, E. N. Ponyavina, R. M. Gadirov, M. G. Kaplunov and T. N. Kopylova, *Spectrochim. Acta, Part A*, 2014, **128**, 137–140.